Biochimica et Biophysica Acta, 455 (1976) 412–432

BBA 77495

CORRELATED X-RAY DIFFRACTION AND FREEZE-FRACTURE STUDIES ON MEMBRANE MODEL SYSTEMS

PERTURBATIONS INDUCED BY FREEZE-FRACTURE PREPARATIVE PROCEDURES

M. J. COSTELLO* and T. GULIK-KRZYWICKI

C.N.R.S., Centre de Génétique Moléculaire, 91190 Gif-sur-Yvette (France)

(Received April 26th, 1976)

SUMMARY

Lipid-water and protein-lipid-water phases have been examined by X-ray methods before and after freezing. Frozen samples have been subsequently fractured and replicated, thus permitting an evaluation of the nature of structural perturbations in samples examined by freeze-fracture electron microscopy. Important results are summarized: (1) Freezing low water content (approx. $< 25\%$) phases causes perturbations in the packing of hydrocarbon chains. The results suggest that freezing liquid paraffin chains produces a condensed "glass-like" packing. (2) Additional perturbations occur in high water content samples. After freezing, much smaller lamellar repeat distances, intense ice reflections, and extensive perturbations of fracture faces are consistant with the expulsion of water from between lamellae. Presence of glycerol generally relieves these perturbations but in some cases introduces additional lattice disorder. (3) Surprisingly, cooling by a stream of cold N_2 gas (−140 °C) produces qualitatively the same results as rapid cooling in liquid Freon-22 (−160 °C). (4) Complex perturbations occur in phases containing integral membrane proteins. Interesting results have been obtained with cytochrome b_5-lecithin lamellar associations which display both smooth and rough fracture faces without clearly defined particles.

INTRODUCTION

Present concepts about the organization of biological membranes are to a large extent based on the information obtained by freeze-etching electron microscopy. This technique, which is currently one of the best for studying membrane molecular organization is, however, limited by its low resolution and by our imprecise knowledge about the perturbations of the original organization which may occur

* Present address: Department of Anatomy, Duke University Medical Center, Durham, N.C. 27710, U.S.A.

during quenching and fracturing of the samples and during the replication of fractured surfaces.

Because the molecular organization in frozen samples is critically dependent on the quenching step, we began a systematic study of the effects of freezing on model systems. In this article we describe the results for lipid-water and protein-lipid-water phases in which, unique to this study, X-ray diffraction patterns before and after freeze quenching were recorded for identically the same samples which were subsequently fractured and replicated. These procedures allowed a critical assessment of the type and extent of structural perturbations introduced in the preparation of samples for freeze-fracture electron microscopy and have permitted a direct comparison of the morphological features of fracture faces to the average structural properties revealed by X-ray scattering. Preliminary accounts of this work have been reported previously [1, 2].

MATERIALS AND METHODS

Egg lecithin was prepared according to the method of Singleton et al. [3]. Wheat germ phosphatidylinositol and beef heart cardiolipin were generously provided by Dr. M. Faure (Institut Pasteur, Paris). Total lipid extract from an *Escherichia coli* fatty acid auxotroph grown on elaidic acid was obtained as described previously [4]. Cholesterol was purchased from Sigma. The purity of all lipids used was checked by thin-layer chromatography prior to the preparation of the samples.

Cytochrome *c* was purchased from Sigma (type VI) and used without further purification. Microsomal cytochrome b_5, a kind gift of Drs. Dufourcq, Bernon, and Lussan (Centre de Recherche Paul Pascal, Talance, France), was prepared according to the method of Spatz and Strittmatter [5].

Lipid-water lamellar phases have been prepared by mixing weighed amounts of lipids and water and allowing sufficient time for equilibration. In the case of phases containing two different lipids, the lipids were first dissolved in an organic solvent in which both lipids were perfectly soluble, then the solvent was evaporated. This procedure was repeated three times to ensure complete mixing. A lipid-water hexagonal phase was obtained by precipitation of the calcium salt of cardiolipins (beef heart) from its water dispersion using 0.01 M $CaCl_2$ [6]. Cytochrome *c*-phosphatidylinositol was prepared by precipitation as described previously [7]. Associations between cytochrome b_5 and lecithin were prepared as described by Dufourcq et al. [8]. Ordered lamellar phases were obtained by high speed centrifugation of the vesicular material followed by controlled dehydration. The extent of ordering was evaluated at different stages of dehydration by small-angle X-ray diffraction.

Our experimental set-up used for recording low temperature X-ray diffraction patterns of the samples is shown in Fig. 1. The sample was placed on a Balzers gold planchett commonly used in freeze-fracture experiments. The planchett was supported by a small metal holder fixed on a glass capillary whose position was controlled by a micromanipulator. The sample temperature was controlled by a laminar stream of cold N_2 gas delivered by an apparatus developed for maintaining small samples at constant, very low temperatures for extended periods of time. The temperature of the stream of N_2 could be varied from about liquid nitrogen temperature up to

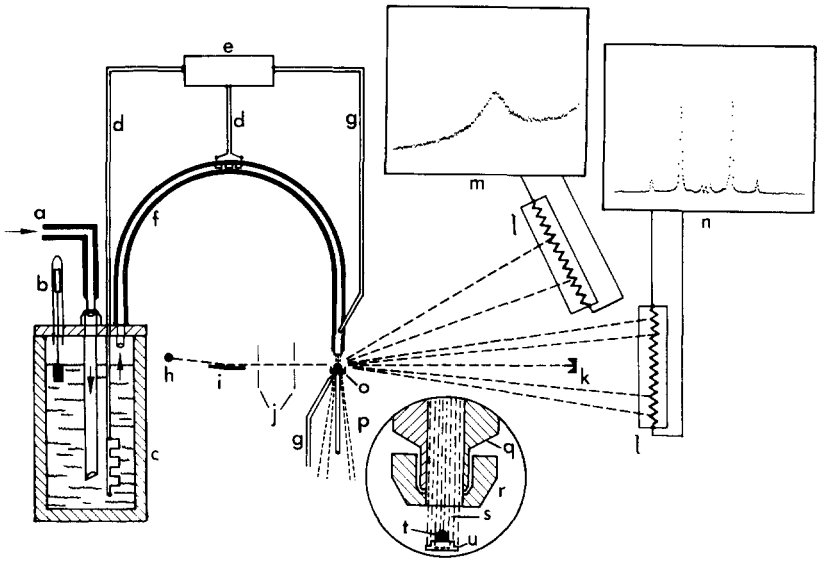

Fig. 1. Schematic of experimental set-up. (a) liquid nitrogen input; (b) level indicator; (c) constant level dewar; (d) heaters; (e) heater control; (f) flexible dewar transfer tube; (g) thermocouples; (h) X-ray source; (i) focusing mirror; (j) slits; (k) beam attenuator; (l) linear position-sensitive detectors; (m) wide-angle output from multichannel analyzer; (n) low-angle output from multichannel analyzer; (o) sample support cup; (p) glass rod; see insert for (q) cryostat output tip; (r) heated cap to eliminate frost; (s) laminar flow of gaseous nitrogen; (t) sample; (u) Balzers gold planchett. The three small peaks in the center of the low-angle pattern (n) represent the scatter around the Ni foil beam attenuator (k) and the scatter through the beam attenuator. Subsequent X-ray patterns will only show one half of the centrosymmetric low-angle patterns.

0 °C with the precision better than ± 1 °C. A detailed description of this apparatus is given elsewhere [9].

On our set-up the sample was placed about 5 mm below the tip of flexible dewar (see insert in Fig. 1). The temperature of the sample was estimated from thermocouple measurements of the temperature of the stream of N_2 at the end of flexible dewar and from the small metal holder supporting the gold planchett. The difference between these two measurements never exceeded 5 °C. The source of X-rays was an Elliot GX-6 rotating anode generator operated at 25 kV and 25 mA. A nickel filtered, line focused beam (approx. 0.1–0.2 mm width at the sample) was produced using a single gold-coated mirror and slit collimation. Position-sensitive detectors [10] were used for recording low- and wide-angle diffraction patterns. Freeze-fracturing was performed using a Balzers 301 freeze-etching unit with Pt-C shadowing. The replicas were observed in Philips 301 electron microscope. Optical diffraction was performed on selected electron micrograph negatives.

Each sample was examined following the procedure outlined in Fig. 2. After determining by X-ray diffraction of the sample in a sealed sample holder that equilibrium had been reached, the holder was opened and small portions of the sample were placed on gold planchetts. Some samples were subsequently quenched in Freon-22 (−160 °C) and others were examined at room temperature to insure that

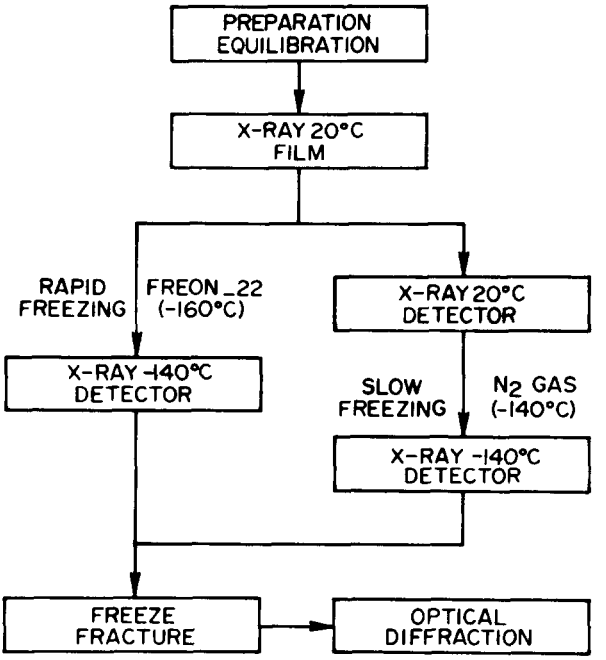

Fig. 2. Outline of experimental procedure. See text for explanation of steps.

no changes had occurred during the preparation of the samples. These room temperature samples were then cooled by directing the stream of cold N_2 gas (−140 °C) onto the sample (Fig. 2, slow cooling). Under this condition the rate of cooling is between 100 and 300 °C/s (Costello and Keira, unpublished) which is approximately one order of magnitude slower than the freezing in liquid Freon-22 (Bank and Mazur, personal communication). After recording the X-ray diffraction pattern at low temperature, the slowly cooled sample was stored in liquid nitrogen. Each Freon-frozen sample was then placed on the small metal holder separately and examined at the same low temperature (−140 °C). The temperature of the N_2 stream was maintained at −140 °C in order to eliminate frozen Freon from the surface of the samples. The samples were subsequently fractured and replicated. Care was taken to include samples in each freeze-fracture run which had well known fracturing properties. This minimized potential artifacts of any particular fracturing and shadowing condition. The organic material was dissolved in ethanol (lipid-water phases) or digested with Chlorox (lipid-protein-water phases). The freeze-fracture images presented here all have the shadow direction approximately from the lower left to the upper right. All micrographs are × 75000.

RESULTS AND DISCUSSION

Comparisons of X-ray diffraction from samples before and after freezing permit the assessment of the structural changes induced by the freezing process. Low-angle diffraction is used here to follow changes in the long range organization of samples,

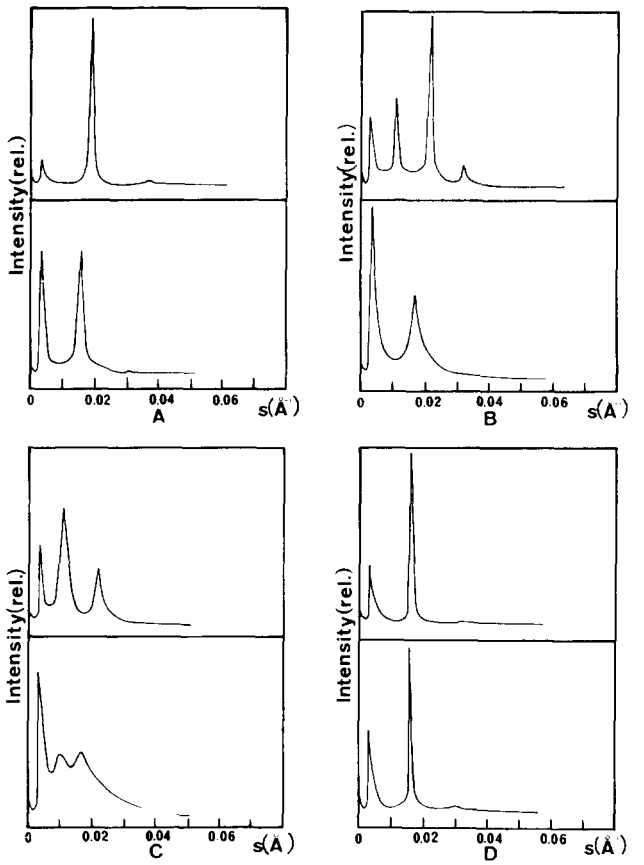

Fig. 3. Low-angle X-ray diffraction from lipid-water phases. (A) L_α phase of lecithin-phosphatidylinositol (50 : 50 by weight) with 16 % water, (B) with 50 % water, and (C) with 62 % aqueous solution containing 20 % glycerol (by weight); (D) L_β phase of lipids extracted from an *E. coli* mutant grown on elaidic acid with 8 % water. In each case the upper patterns were taken at room temperature and the lower ones at −140 °C after freezing in Freon-22 (−160 °C). Lattice spacings are given in Table I. The abscissa $s = 2 \sin \theta/\lambda$ where θ is the half-scattering angle and λ = wavelength (1.5418 Å).

specifically, the change of dimensions of lattices and their disordering (as judged from the broadness of X-ray reflections). Wide-angle X-ray diffraction is mainly used to follow the perturbations in the packing of the lipid hydrocarbon chains. It also gives information about the presence or absence of ice which has characteristic strong reflections between 3 and 4 Å (see Fig. 5).

Lipid-water phases

(1) *Perturbations in the long range organization.* Low-angle X-ray diffraction data on lipid-water systems are presented in Figs. 3 and 4 and in Table I. All lipid-water lamellar phases with a disordered conformation of lipid hydrocarbon chains (α-type conformation; model given in Fig. 5) display very similar changes after freezing. The sample of egg lecithin: phosphatidylinositol (50: 50 by weight) was studied most extensively because for this mixture the α-type lamellar phase was

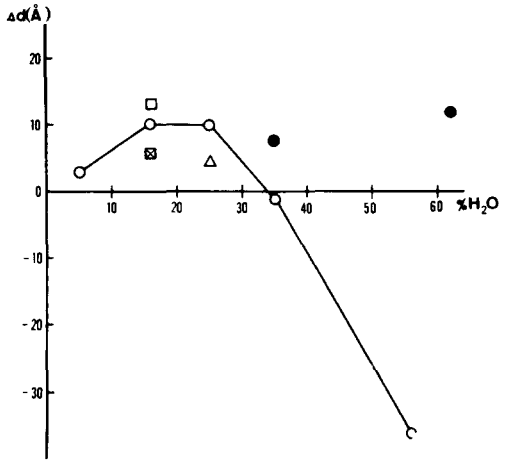

Fig. 4. Changes in lattice repeat distances (Δd) resulting from freezing samples of varying water content in Freon-22 (−160 °C). ○, lecithin-phosphatidylinositol (50 : 50 by weight); ●, in the presence of glycerol; □, egg lecithin without and with glycerol ⊕, egg lecithin-cholesterol (2 : 1, w/w); △, phosphatidylinositol. Positive numbers represent expansion and negative numbers, contraction.

TABLE I

X-RAY LATTICE DIMENSIONS OF LIPID-WATER AND PROTEIN-LIPID-WATER PHASES

Low-angle X-ray diffraction results at room temperature (20 °C) and at −140 °C after freezing in Freon-22 (−160 °C) or a stream of N_2 gas (−140 °C). Phase types are pictured in Fig. 5.

Sample	Type of phase	Lattice spacings (Å)*		
		20 °C	−140 °C	
			Freon-22	N_2 gas
Lecithin-phosphatidylinositol- 5 % water	Lα	52	56	55
Lecithin-phosphatidylinositol-16 % water	Lα	54	64	63
Lecithin-phosphatidylinositol-25 % water	Lα	54	64	63
Lecithin-phosphatidylinositol-35 % water	Lα	59	58	57
Lecithin-phosphatidylinositol-35 % (water+glycerol)	Lα	58	65	64
Lecithin-phosphatidylinositol-56 % water	Lα	95	59	60
Lecithin-phosphatidylinositol-62 % (water+glycerol)	Lα	94	106	107
Lecithin-16 % water	Lα	53	67	66
Lecithin-16 % (water+glycerol)	Lα	52	66	66
Lecithin-cholesterol-16 % water	Lα	54	60	59
Phosphatidylinositol-25 % water	Lα	52	57	57
E. coli lipids	Lβ	62	63	62
Calcium-cardiolipins (excess water)	Hα	50	54	52
Cytochrome *c*-phosphatidylinositol (excess water)	–	81	75	75
Cytochrome *c*-phosphatidylinositol (excess water with 20 % glycerol)	–	80	88	87
Cytochrome b_5-lecithin	–	209	**	–

* The estimated accuracy of all lattice spacings is about ±1 Å.

** Single broad peak at 75 Å (Fig. 13B) cannot be interpreted in terms of a lamellar lattice repeat without additional information.

present over a wide range of water concentrations. At low water content (up to 30 % by weight) appreciable expansion of the lamellar lattices was observed without noticable changes in the long range order, as judged from the sharpness of lamellar reflections after freezing (Fig. 3A). At intermediate water contents (30–40 %) the changes in dimensions and ordering of lattices are small. At high water content (more than 50 % water) large contractions of the lattice dimensions are observed together with broadening of reflections indicating the presence of significant amounts of lattice disorder (Fig. 3B).

The contraction of lamellar lattices in the presence of large amounts of water is probably caused by a decrease in the thickness of water layers between the lipid lamellae induced by the growth of large ice crystals. This explanation is confirmed by the results obtained in the presence of glycerol (which limits the rate of the crystal growth). If water is replaced by the solution containing 20 % glycerol, only expansion of lamellar lattices are observed for all water concentrations studied. Glycerol can induce some small changes in the lamellar lattice dimensions and order at room temperature (for example, compare Figs. 3B and 3C), particularly in the case of charged lipids (data not shown). Increased disordering is observed after the freezing of samples containing glycerol (see Fig. 3C).

The observed expansion of the lamellar lattices after freezing in the presence of glycerol and in the case of the samples containing less than 30 % water must be due in part to the increase in thickness of lipid lamellae, since the contribution of water cannot account entirely for the observed expansions*. Increased thickness of the lipid leaflets must be accompanied by the changes in the packing of the lipid hydrocarbon chains. It is important to note that, on one hand, the lipid-water lamellar phase displaying an ordered conformation of the hydrocarbon chains (β-type conformation, see Fig. 5) does not show any appreciable change in lattice dimension or ordering of the lamellar lattice after freezing (Table I and Fig. 3D), and, on the other hand, a lipid-water two-dimensional hexagonal phase displaying disordered conformation of the hydrocarbon chains (phase Hα in Fig. 5 and see ref. 6) does show an expansion of the hexagonal lattice (Table I). The changes in the packing of the lipid hydrocarbon chains after freezing are further described on the basis of the wide-angle X-ray diffraction data (see below).

(2) *Perturbations in the packing of the lipid hydrocarbon chains.* Wide-angle X-ray diffraction data on different lipid-water systems are presented in Fig. 5 and in the Table II. The most striking observation in the case of phases displaying disordered conformations of the hydrocarbon chains (Lα and Hα; see Fig. 5) is the displacement of their characteristic 4.5 Å broad band to a 4.2 Å broad reflection. (See Fig. 5 for method of measurement of wide-angle spacings and Table II for precise values.) This is a clear indication of the changes in the packing of hydrocarbon chains towards more closely packed but still quite disordered conformation. The fact that both Lα and Hα phases after freezing give almost identical 4.2 Å broad reflections indicates that the conformation of the hydrocarbon chains after freezing is closer to a "glass-like" packing than to a highly ordered β-type arrangement (Fig. 5). The β-type conformation is incompatible with the long range organization of the lipids in Hα phase,

* The volume expansion of water to ice at 0 °C is about 1.09 [11]. If all the water between the lamellae is assumed to behave as free water, the linear expansion of water for the case of 25 % water by weight (water layer approx. 6 Å) would be only 0.2 Å.

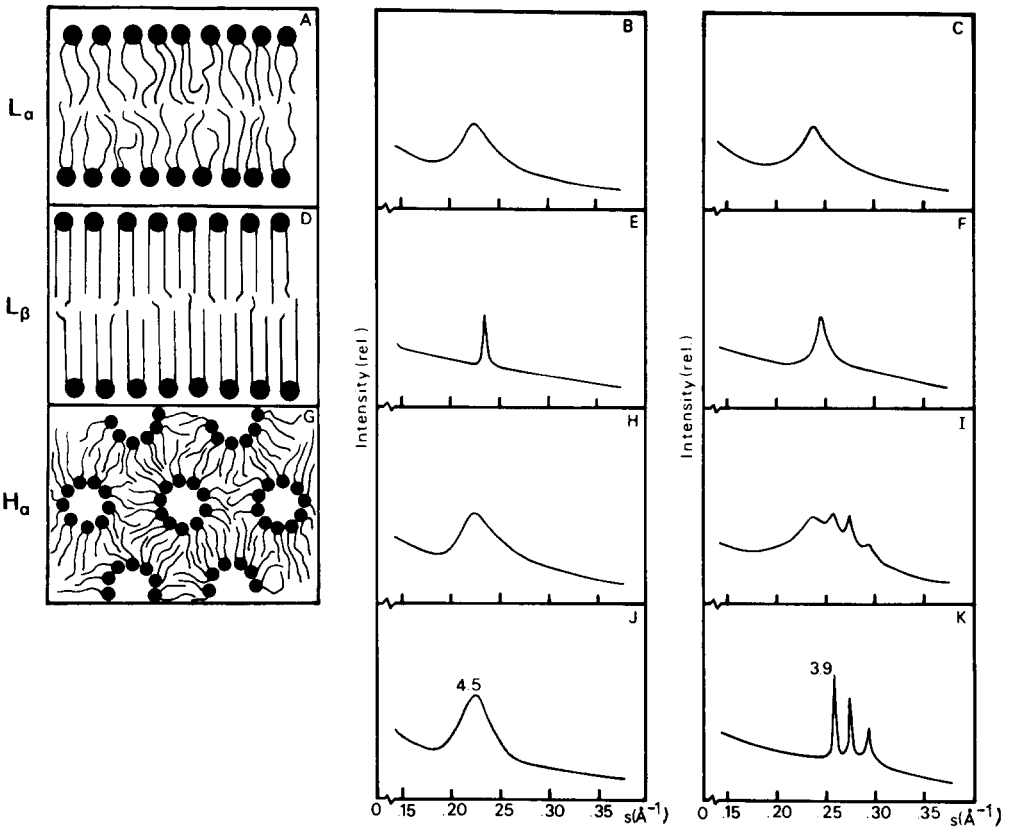

Fig. 5. Wide-angle X-ray diffraction patterns from lipid-water phases. (A), (B) and (C) illustrate behavior of L_α phases of lecithin-phosphatidylinositol (50 : 50 by weight) with 5 % water; (D), (E) and (F) of L_β phase of *E. coli* lipid extract with 8 % water; (G), (H) and (I) of H_α phase of calcium precipitated cardiolipins in excess water. (J) and (K) spacing standards *n*-decane (4.50 Å) and ice in frozen 15 % glycerol solution (3.90 Å), respectively. Patterns in column (B), (E), (H) and (J) were recorded at room temperature and in column (C), (F), (I) and (K) at −140 °C after freezing in Freon-22 (−160 °C). The drawing in (G) is a cross-section of hexagonally packed water cylinders (see ref. 6). The pattern in (I) contains strong ice peaks superimposed on the broad diffraction peak. The spacing values derived from these measurements are relative since they depend on the assumed standards used to calibrate a portion of the detector wire. The sharp peaks for ice are (K) consistant with ice spacings of 3.90, 3.67 and 3.44 Å [12].

formed from two-dimensionally packed lipid cylinders (see model in Fig. 5). Freezing of the Lβ phase introduces only a small change in the packing of the hydrocarbon chains: the characteristic 4.2 Å sharp reflection is replaced after freezing by slightly broader 4.1 Å reflection (Table II).

The above described changes in the packing of lipid hydrocarbon chains can be correlated with the observed lattice expansions for all lipid-water phases in which no local changes of the chemical composition of the phase is observed after freezing. Closer packing of the lipid hydrocarbon chains induces an increase of the thickness of the lipid leaflet leading to the expansion of the lattices. The correlation between changes in packing of lipid hydrocarbon chains and the changes of the lamellar lattice dimension is further shown by the data on the samples containing

TABLE II

WIDE-ANGLE X-RAY RESULTS FOR LIPID-WATER PHASES AND PROTEIN-LIPID-WATER PHASES

Positions of wide-angle X-ray peaks are averages for different phases (see Fig. 5). Relative measurements using standards *n*-decane (4.50 Å) and ice in frozen 15 % glycerol (3.90 Å). Estimated precision is ±0.03 Å.

Phase	Wide-angle spacings (Å)		
	20 °C	−140 °C	
		Freon-22	N_2 gas
Lα	4.44	4.14	4.15
Lβ	4.19	4.06	4.08
Hα	4.46	4.19	4.18
Cytochrome *c*-phosphatidylinositol (excess water)	4.44	4.19	4.20
Cytochrome *c*-phosphatidylinositol (excess water with 20 % glycerol)	4.38	4.15	4.15
Cytochrome b_5-lecithin	–	4.15	–

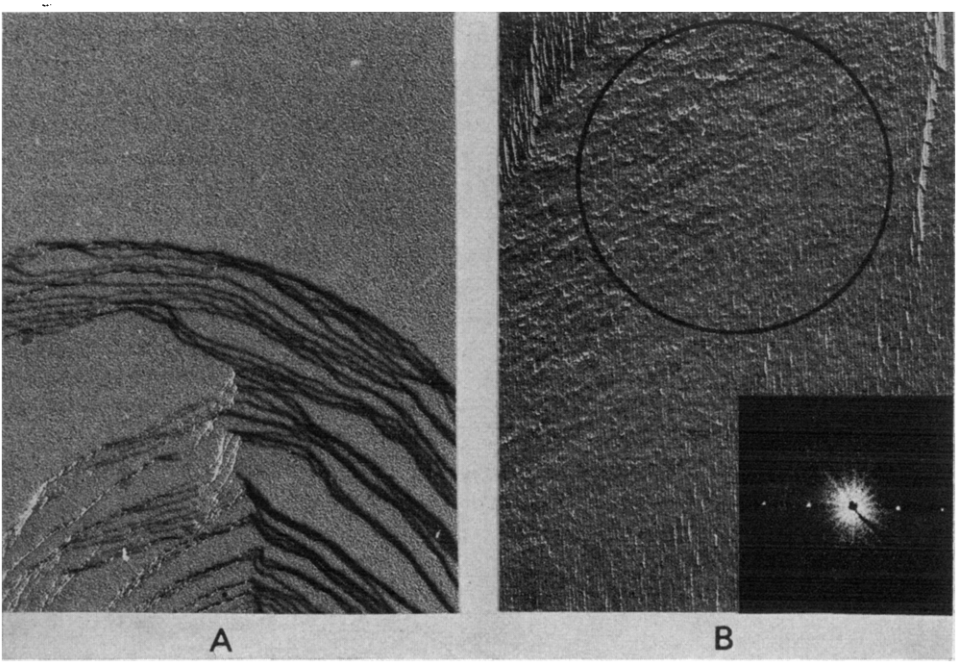

Fig. 6. Freeze-fracture micrographs of the L_β phase. (A) Oblique fracture showing smooth fracture faces. (B) Fracture perpendicular to stacked lamellae; optical diffraction pattern (insert) is from the micrograph negative in the area marked by the circle. The size of the beam indicated by the circle (intersecting about 100 layers here) was used in all succeeding optical diffraction patterns. The lattice repeat distance indicated in the diffraction pattern from the center to the discrete spots on etiher side was set equal to that measured from X-ray patterns of the frozen sample (62 Å); this forms a relative scale for measuring spacings from other optical diffraction patterns. Sample was frozen in a stream of N_2 gas (−140 °C); samples rapidly cooled in Freon-22 give nearly identical results. This sample was chosen as a standard because its lattice showed the highest perfection.

cholesterol. Smaller expansion of the lamellar lattice in the presence of cholesterol, 6Å instead of 14 Å, (see Table I) is accompanied by smaller changes on freezing of the packing of the lipid hydrocarbon chains as judged from the wide-angle scattering. The broad reflection after freezing is reproducible at a larger spacing (approx. 0.05 Å) than the average value for lecithin without cholesterol.

(3) *Morphological Perturbations.* In order to discuss rigorously the morphological perturbations of the phases we must compare electron micrographs of a given sample to the micrographs of a standard displaying the same type of lattice but for which one can assume on the basis of independent experiments that no perturbation of lattice dimensions and ordering take place during freezing. According to our X-ray diffraction data only the L_β-type lamellar phase satisfies these requirements. The electron micrographs of the L_β phase are shown on Fig. 6. The images of the fractures perpendicular to the plane of stacked lamellae show nearly perfect regularity in the packing; this is particularly clear from the sharpness of the optical diffraction spots corresponding to these images (see Fig. 6B). For fractures not perpendicular to the lamellae, extended smooth fracture surfaces are observed (Fig. 6A).

In the absence of glycerol the only lamellar phases producing pictures nearly identical to the standard defined above are those which contain very small amounts of water (less than 10 %; Figs. 7A and 7B). Samples containing larger amounts of water can show some unusual deformations in the lamellar packing (Fig. 7C). These defect structures may be due to the expansion of lamellar lattices leading to the formation of lattice defects. It is also possible that freezing is enhancing some preexisting lattice defects characteristic of the smectic phases; this will be discussed in detail elsewhere [13]. Different morphological perturbations affecting the smoothness of fracture faces are occasionally seen on some replicas of samples at intermediate water content (Fig. 7D). They have a similar appearance but are less pronounced than those which occur in samples containing greater amounts of water (more than 40 % water). In these high water content samples very striking morphological perturbations are observed (Fig. 8A). These perturbations seem to originate from the growth of ice crystals between lamellae, leading to the formation of small "ice pockets" which can clearly be seen in electron micrographs of perpendicular fractures (Fig. 8B). "Ice pockets" indicate the location of large ice crystals which are formed from the water separating lipid leaflets (see model in Fig. 8C). This leads to the contraction of the average thickness between lamellae due to the decreased thickness of water layers separating the lipid lamellae.

Replacement of water by a 20 % glycerol solution alleviates this type of morphological perturbation. Most of the images for the samples containing glycerol are similar to the standard L_β phase: good order in the stacking of lamellae as seen on the fractures perpendicular to the planes of lamellae (and the corresponding optical diffraction) and extended smooth surfaces for obligue fractures (Compare Fig. 6 to Fig. 9). Somewhat different freeze-fracture images are observed in the case of egg lecithin-water lamellar phases. The extended fracture planes are not totally smooth but show some irregular random corrugations (Figs. 10A and 10B). This type of perturbation is probably due to the formation during freezing of small regions containing ordered hydrocarbons chains (β-type). For example, when the same samples are cooled very slowly to −20 °C, ordered two-dimensional lattices are formed from alternating regions of ordered and disordered hydrocarbon chains

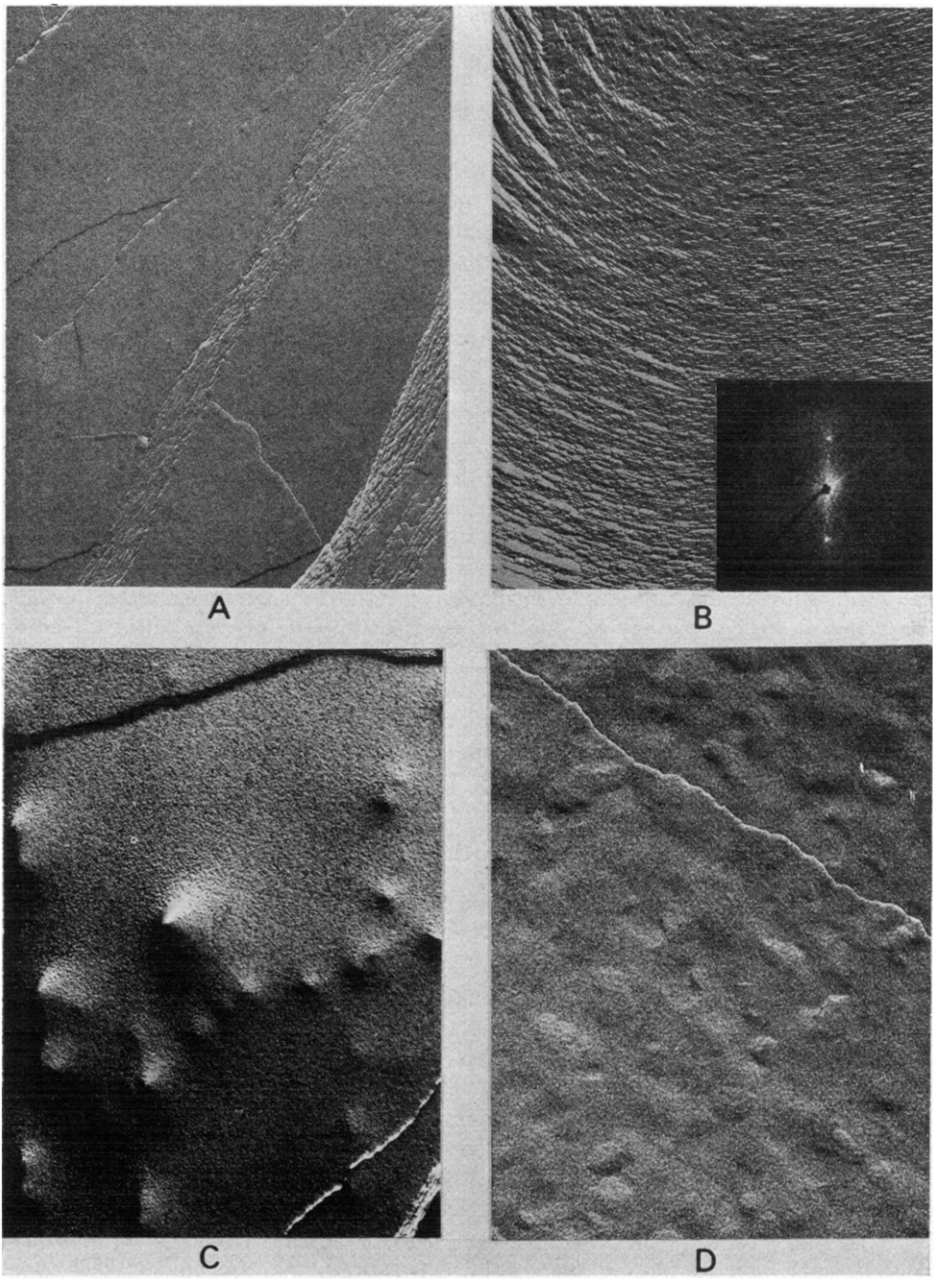

Fig. 7. Freeze-fracture of L_α phases of low water content. Lecithin-phosphatidylinositol (50 : 50 by weight). (A) Oblique and (B) perpendicular fractures, with 5 % water. Optical diffraction (B insert) shows well defined spots of a 53 Å spacing. (C) Oblique fracture with 16 % water showing peaks related to the defect structures of the multilamellar systems. Although present in some form in most lamellar phases, these perturbations are distinct from those related to freeze-fracture preparative procedures [13]. (D) Oblique fracture with 25 % water.

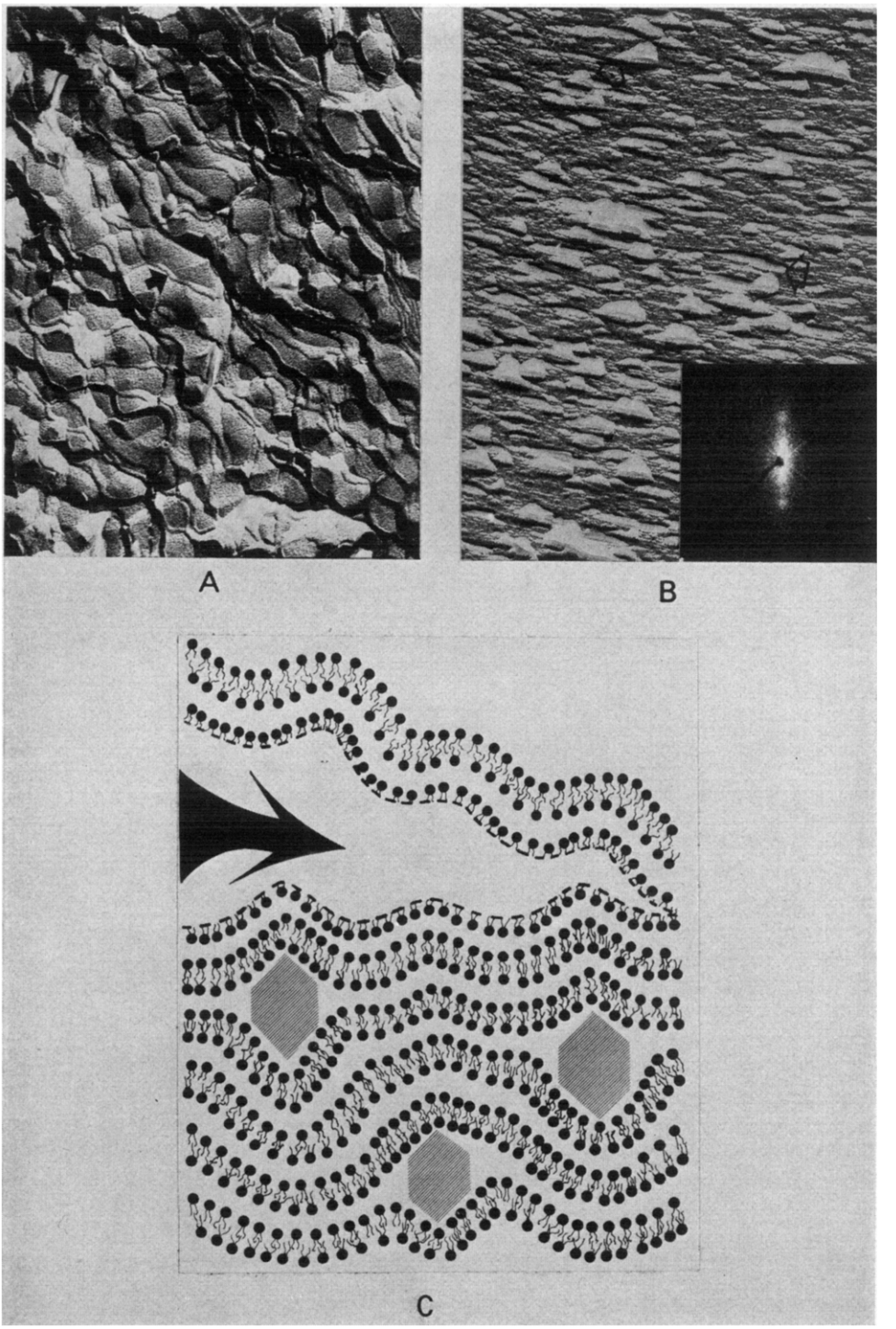

Fig. 8. Freeze-fracture of L_α phase of high water content. Lecithin-phosphatidylinositol (50 : 50 by weight) with 56 % water. (A) Oblique fracture showing stricking angular perturbations which reveal small patches of smooth fracture faces. Arrow denotes a fracture step of one bilayer thickness. (B) Perpendicular fracture showing stacked lamellae interrupted randomly with objects believed to be ice pockets (arrows). (C) Interpretation of micrographs where ice pockets (hexagons) are seen to perturb the surface exposed by the fracture (arrow). The accumulation of water into the ice pockets causes an average reduction in layer spacing after freezing from 95 to 59 Å and a disruption of the regular lattice; both features are shown in the optical diffraction (B insert).

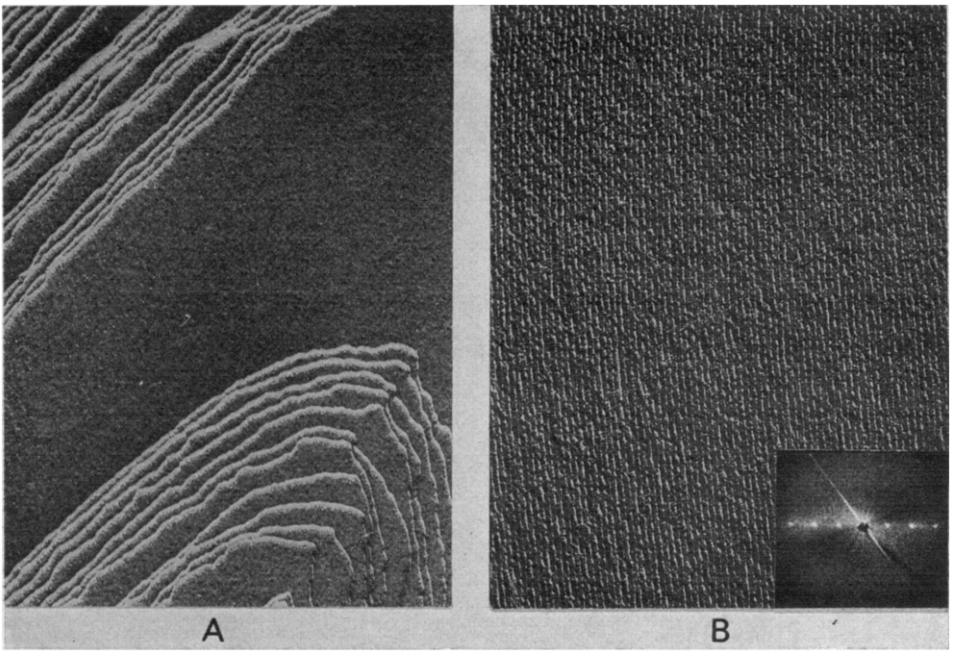

Fig. 9. Freeze-fracture of L_α phase of high water content in the presence of glycerol. Lecithin-phosphatidylinositol (50 : 50 by weight) with 62 % aqueous solution containing 20 % glycerol (by weight). (A) Oblique fracture showing smooth surfaces. (B) Perpendicular fracture showing uniform stacking of lamellae without perturbations. Optical diffraction (insert) shows a well defined lattice of about 114 Å spacing.

(Figs. 10C and 10D; see refs. 14 and 15). Conventional freezing (Freon-22) is, in the case of this egg lecithin-water L_α phase, not rapid enough to prevent a segregation of the lipid into ordered and disordered domains, but the distribution of these domains is not regular (Fig. 10A). More regular distributions are observed after slower freezing in the stream of cold N_2 gas (Fig. 10B) but still not as regular as in the case of samples cooled very slowly (Fig. 10C).

Protein-Lipid-Water Phases

(1) *Cytochrome c-phosphatidylinositol-water lamellar phase.* As has been shown previously [7], the interactions between cytochrome *c* and phosphatidylinositol are in this phase mainly electrostatic in nature. Any perturbations of the lipid hydrocarbon core are therefore very small. The partial thickness of the lipid leaflet in this phase is the same as in pure phosphatidylinositol-water lamellar phases [7]. One could infer from these results that the perturbations of the hydrocarbon region induced by freezing this type of protein-lipid-water phase would be similar to those observed for corresponding lipid-water phases. Wide-angle X-ray diffraction results shown in Fig. 11B and in Table II confirm this hypothesis. The packing of the lipid hydrocarbon chains is equally perturbed in both cases. The perturbations of the lamellar lattice dimensions are, however, quite different. As can be seen from Fig. 11 and from the Table I, a contraction of the lamellar lattice is observed in the presence of cytochrome *c* while an expansion of the lamellar lattice is observed for the phos-

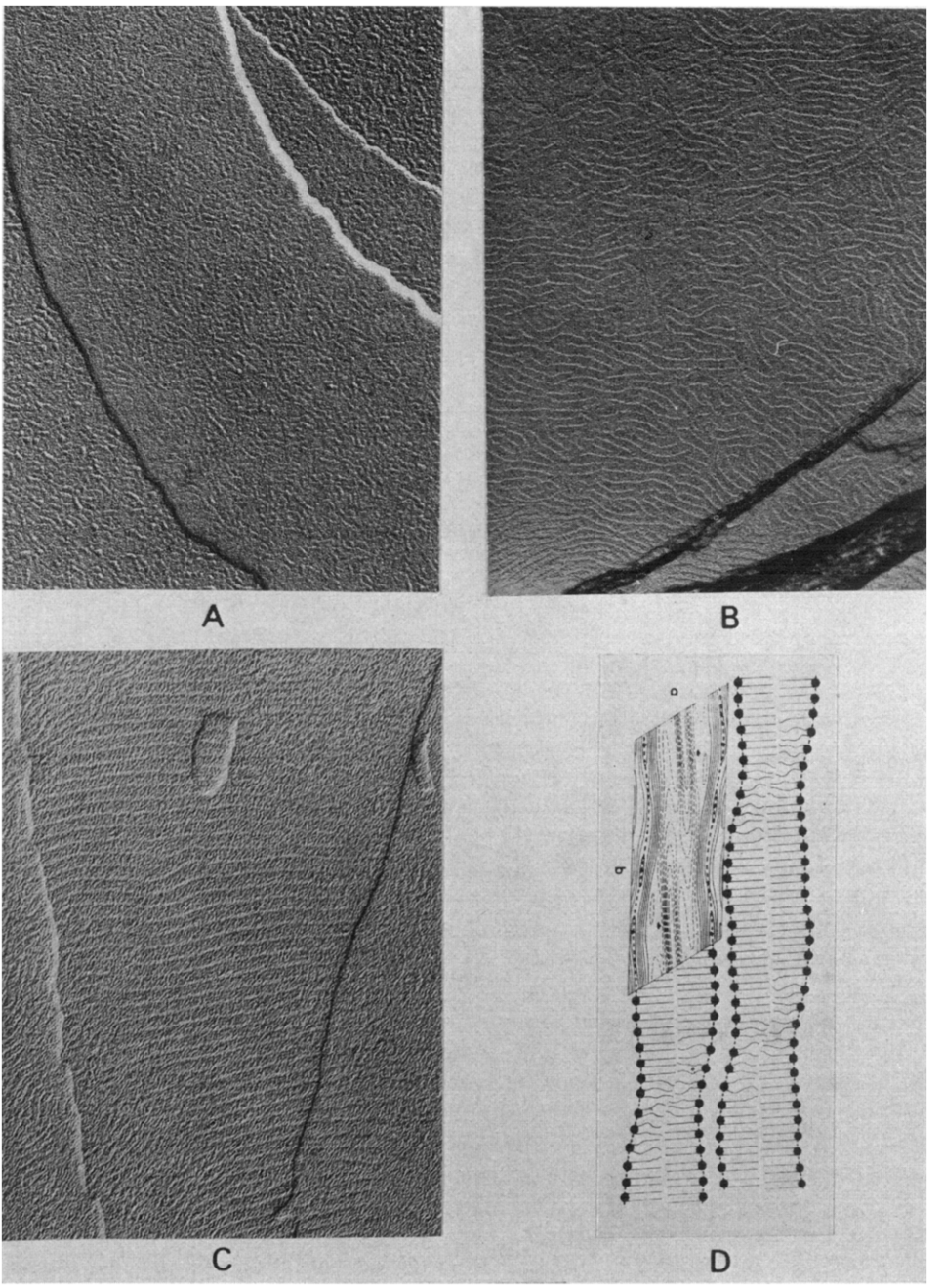

Fig. 10. Freeze-fracture of L_α phase of egg lecithin as a function of freezing rate. Water content 16 %. (A) Freeze-quenching in Freon-22 (−160 °C). Notice "worm-like" textured pattern on extended fracture surfaces. (B) Freezing in stream of N_2 gas (−140 °C). Notice in fracture faces that small domains of parallel ridges have formed. (C) Gradually cooled (about 1 °C/min) to −20 °C. Regular two-dimensional array ($P_{\alpha\beta}$ phase) in plane of bilayers has formed. (D) Molecular interpretation of the $P_{\alpha\beta}$ phase. The electron density contour map derived from an X-ray diffraction analysis is shown (from ref. 14).

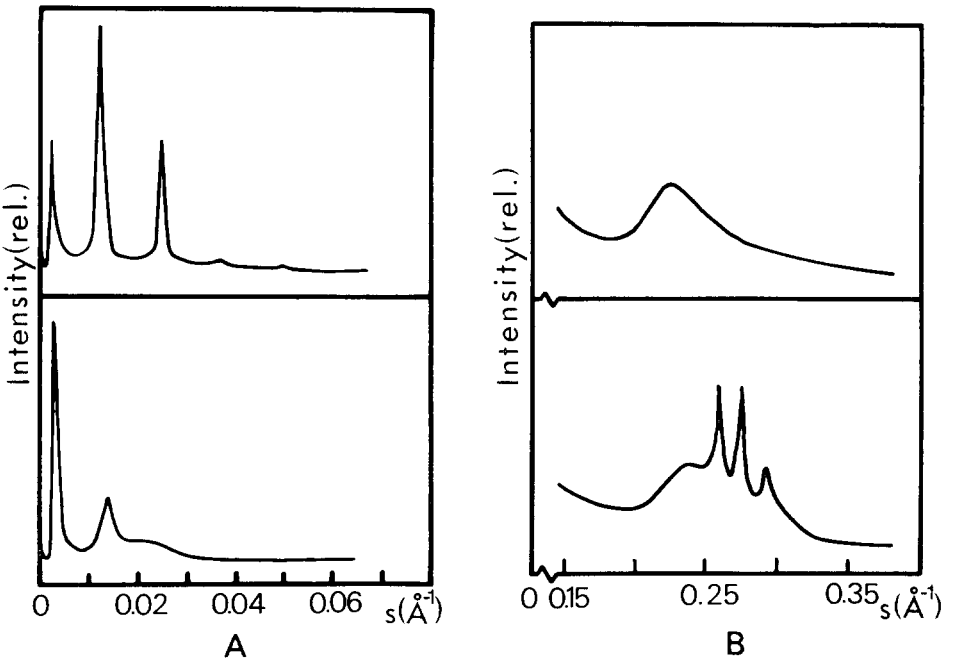

Fig. 11. See opposite page for legend.

phatidylinotitol-water lamellar phase containing a similar amount of water. That the contraction of the lamellar cytochrome *c*-phosphatidylinositol phase is caused by the expulsion of water from the phase is shown by the results obtained on the samples containing glycerol. When the phase is precipitated in the presence of glycerol, an expansion of the lattice is observed (Table I). The difference in the lattice dimensions after freezing of the samples in the presence and in the absence of glycerol (88 and 75 Å, respectively) suggests that probably most of the water is expulsed from the phase without glycerol. Assuming that the expansion of the lamellar lattice observed in the presence of glycerol (8 Å) is mainly due to the increased thickness of the lipid bilayers, one can estimate the value of the repeat distance of the rapidly frozen sample without glycerol at room temperature: 75—8 = 67 Å, the value which is very close to the 68 Å observed for completely dry sample at room temperature [7]. The above hypothesis aids in the interpretation of the images obtained for rapidly cooled cytochrome *c*-phosphatidylinositol-water samples. Both show smooth fracture faces in oblique fractures. Glycerol-containing samples show very minor morphological perturbations in the stacking of lamellae in perpendicular fractures (Fig. 11D), while the samples without glycerol show extended ice domains (Fig. 11C). These domains seem to surround extended lamellar regions rather than be randomly distributed between individual lamellae (as in the case of lipid-water lamellar phases containing large amounts of water; see Fig. 8). It is possible that, due to the electrostatic interactions between positively charged cytochrome *c* and negatively charged phosphatidylinositol, the formation of "ice pockets" in between the lamellae is more difficult than the expulsion of the water from between the lamellae into macroscopic regions which separate protein-lipid-water lamellar domains. It is, however, also

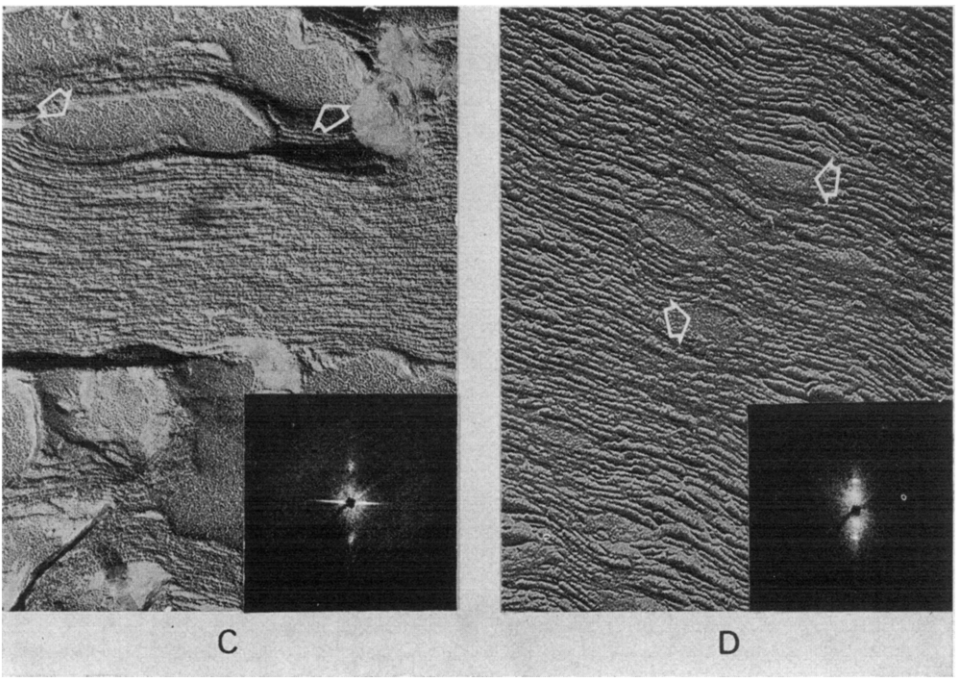

Fig. 11. X-ray and freeze-fracture results for cytochrome *c*-phosphatidylinositol-water lamellar phase. (A) Low-angle X-ray patterns of room temperature precipitate (upper pattern, 81 Å lattice repeat) and same sample frozen in Freon-22 (lower pattern, 75 Å lattice repeat). Notice the lattice has become slightly disordered. (B) Wide-angle X-ray at room temperature (upper pattern, peak spacing 4.4 Å) and same sample frozen in Freon-22 (lower pattern, spacings 4.2 Å for the broad peak). The sharp peaks are due to ice crystals (see Fig. 5K) which are prominant because the precipitate is formed in excess water. (C) Perpendicular fracture showing stacked lamellae and very large ice crystallites (arrows). Optical diffraction (insert), spacing 75 Å. (D) Perpendicular fracture for precipitate formed in the presence of glycerol (20 % by weight). Notice much smaller ice pockets (arrows) randomly interspersed between lamellae. Optical diffraction (insert), spacing 96 Å.

possible that the exclusion of water from this phase is at least partly caused by the freezing of the excess of water present in the precipitate, which may lead to the draining of water from the pure phase.

(2) *Cytochrome b_5-egg lecithin lamellar phases.* Associations between cytochrome b_5 and egg lecithin were obtained by incubation of very small lecithin vesicles (about 300 Å diameter) with soluble aggregates of cytochrome b_5. Under this condition, the cytochrome b_5 is probably associated exclusively with the external half of lecithin vesicles [8]. Ordered lamellar phases were obtained by high speed centrifugation (4 h at $350000 \times g$) of these vesicles, followed by controlled drying of the pellet (Fig. 12). Preliminary analysis of the dimensions of lamellar lattices, together with the chemical composition of the phases, indicate that the partial thickness of the components corresponds to the presence of two lipid bilayers and one protein layer within each repeating unit. This suggests that during multiple fusion of the small vesicles leading eventually to the formation of large lamellar sheets, the asymmetric distribution of cytochrome b_5 is preserved and the final

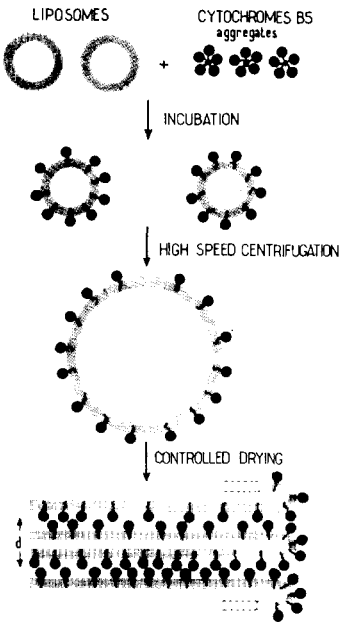

Fig. 12. Preparation of cytochrome b_5-lecithin-water lamellar phases. Solution of liposomes of a nearly uniform size (about 300 Å diameter) are incubated with aggregates of cytochrome b_5 to form vesicles with the protein asymmetrically distributed on the outside [8]. The asymmetric protein distribution may be preserved during the subsequent centrifugation and dehydration steps. The lamellar repeat distances measured by X-ray diffraction (see Fig. 13) are consistent with the molecular arrangement shown (see text).

stacking produces an asymmetric lattice similar to those which have been observed for experimentally stacked asymmetric membrane vesicles (ref. 16 and Fig. 12).

A detailed analysis of the X-ray diffraction and freeze-fracture data on the complex cytochrome b_5-egg lecithin phases observed is still in progress and will be published separately. We will limit ourselves here to reporting the data from one of the lamellar phases to illustrate the extent of lattice disordering induced by conventional freezing. The perturbutions due to the freezing produce changes in the diffraction patterns which are very similar to those observed for rapidly frozen retinal rod outer segments (Corless and Costello, unpublished observations) and peripheral nerve myelin [17]. For all these systems the sharp reflections present at room temperature are replaced by broad peaks in the frozen samples; for the cytochrome b_5 sample, the broad peak is centered at about 75 Å (see Figs. 13A and 13B). It is not clear from the X-ray diffraction data alone whether the low temperature pattern originates from a highly disorganized form of the room temperature lamellar structure or if it originates from some different structures formed during freezing. Freeze-

Fig. 13. X-ray and freeze-fracture results for a cytochrome b_5-lecithin-water lamellar phase. (A) Low-angle X-ray photograph taken with sample in a sealed holder at room temperature. The beam stop has been displaced slightly to reveal the weak second order (arrow) of a lattice of about 200 Å. The remaining strong peaks are orders 3, 4 and 7. (B) Detector X-ray patterns at room temperature (upper) and after freezing in Freon-22 (lower). The peaks in the upper pattern fit on a lamellar lattice

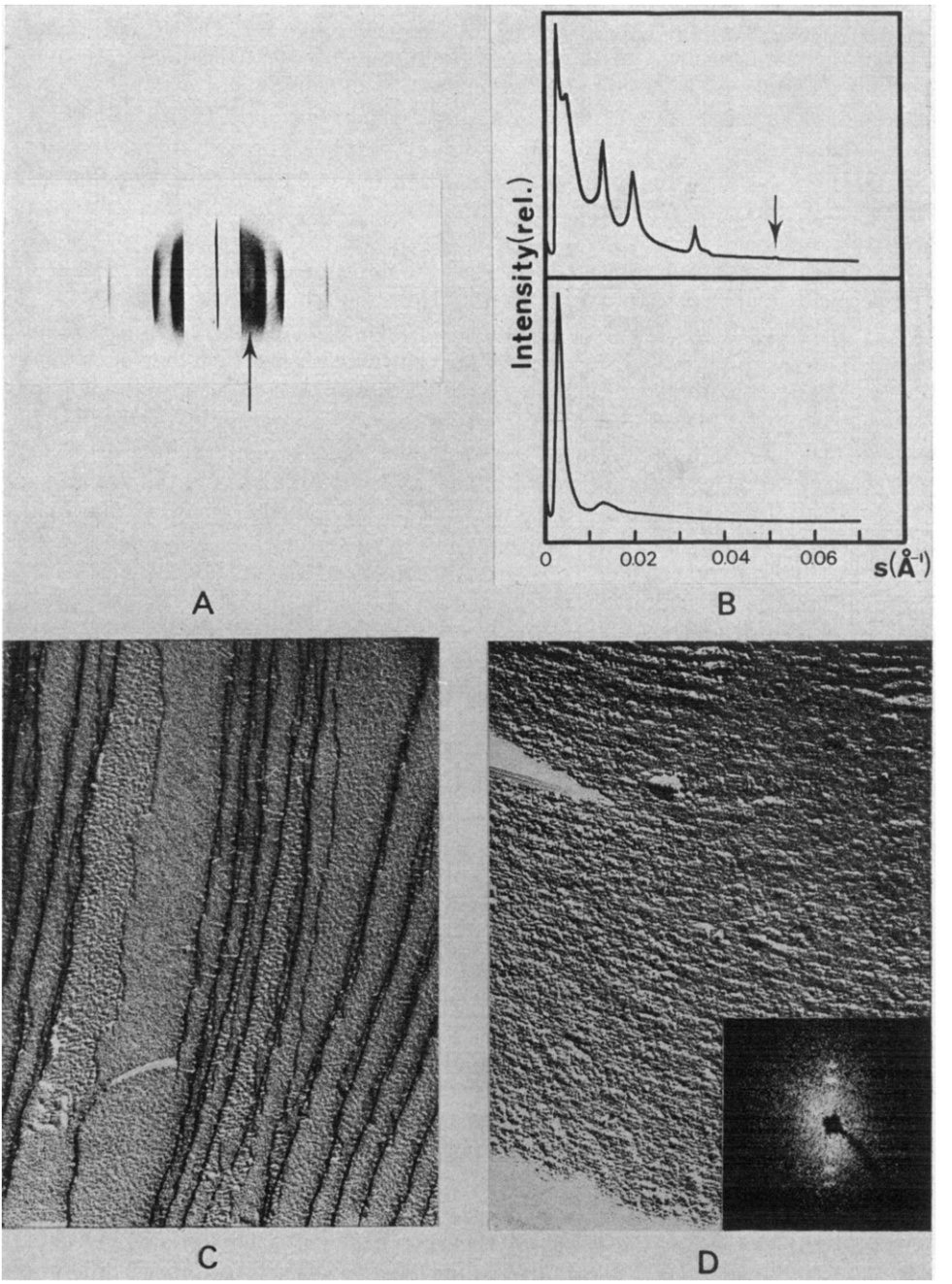

of 200 Å in which the weakest observable peak is the 11th order (arrow). Again the orders 3, 4 and 7 predominate as in A. The single broad peak in the lower pattern, spacing 75 Å, indicates that the regular lattice has been perturbed. (C) Freeze-fracture image (oblique fracture) showing neighboring rough and smooth surfaces. In general the rough surfaces resemble a "cobblestone" pattern and do not contain clearly defined particles. (D) Perpendicular fracture image showing stacked lamellae. It is interesting that optical diffraction (insert) shows three peaks (spacings 51, 69, 102 Å) which can be indexed on a 205 Å lattice similar in size to that found at room temperature (see patterns in A and B).

fracture data, shown in Figs. 13C and 13D, are compatible with the first hypothesis, since images, independent of the type of fractures, show that the sample is homogeneous and formed by a complex association of different types of lamellae characterized by neighboring rough and smooth fracture surfaces. Lattice dimensions from fractures perpendicular to the plane of lamellae (optical diffraction data; Fig. 13D) indicate that the distances between the repeating units are very similar to the repeat distances of the lamellar lattices at room temperature (from X-ray data; Figs. 13A and 13B).

One intriguing problem is the nature of the rough surfaces observed in the non-perpendicular freeze-fracture images. The simplest explanation would be to assume that they originate from fractures through hydrophilic regions containing cytochrome b_5. This would be in good agreement with the fact that such rough fracture planes are totally absent in vesicular cytochrome b_5-lecithin associations obtained after the high speed centrifugation step (Gulik-Krzywicki and Costello, unpublished). It is, however, also possible that these rough fracture planes are reflecting deeper penetration of cytochrome b_5 into lipid bilayers in the phases containing small amounts of water (less than 50 %) or that they may be due to the freezing-induced changes in the penetration of cytochrome b_5. It is even possible that it may reflect some type of very local order-disorder transitions of egg lecithin hydrocarbon chains leading to the formation of small ordered "islands" similar to those described above for some egg-lecithin-water samples (see Fig. 10). Further experimentation employing faster freezing procedures is required before these interpretations can be resolved.

CONCLUSIONS

Correlating the results from X-ray diffraction and freeze-fracture electron microscopy has led to a description of some of the structural perturbations which occur in model systems during freezing. In the L_α phase, most relevant to biological membranes, freezing produces an expansion of the lipid leaflet as a consequence of a condensation of the hydrocarbon chain packing in the planes of the bilayers. An important conclusion is that these perturbations do not produce a lipid phase transition but instead only alter the dimensions of the disordered packing of alkyl chains. A net expansion of the lattice occurs when ice crystal formation is limited, for example, at low water content or in the presence of glycerol. A net contraction can occur when ice crystal growth is extensive resulting in a loss of water from between lamellae.

The structural changes observed by both physical techniques seem in general to be independent of the two cooling rates employed in this study. For example, measured lattice dimensions (Table I) are nearly the same regardless of cooling rate. We conclude therefore that both cooling methods are nearly equivalent in producing perturbations. A possible exception to this generalization occurs with egg lecithin (at low water content; see Fig. 10). In this case the two freezing methods reveal differences in the size of domains of segregated lipid chains. The fact that these local chain segregations can affect the smoothness of fracture phases is especially significant since lecithin is widely used in model system studies.

In some instances the X-ray and freeze-fracture results are confirmatory as is the case for the $L\beta$ phase (Figs. 3D and 6B) where both low-angle X-ray and optical

diffraction of perpendicular fractures indicate that the 62 Å lattice is almost perfectly ordered. In other instances the techniques give complementary information. For example, high water content samples of lecithin-phosphatidyl-inositol frozen in the presence of glycerol (Figs. 3D and 9B) produce broad X-ray diffraction peaks indicating a disordered lattice while the optical diffraction shows a nearly perfect lattice. This implies that the average structure contains a distribution of spacings while in a selected region only a single spacing is represented. Local variations in the distribution of glycerol at the time of freezing or the presence of thermal gradients during freezing may account for these observations.

A similar correlation between the low-angle X-ray and optical diffraction data exists for the cytochrome b_5-lecithin-water phase (Fig. 13). The X-ray patterns indicate a marked disruption of the lattice after freezing which seems less severe in the optical diffraction patterns. However, in this case, because the molecular structure of this phase is unknown, it is not possible to assess the extent of molecular rearrangements caused by freezing. Without the low temperature X-ray results, it would be tempting but premature to propose molecular interpretations about the interaction of cytochrome b_5 with the hydrophobic region of the bilayers. A detailed analysis of such systems containing membrane-bound proteins must be deferred until faster freezing methods which minimize the perturbations described here have been perfected. Several ultra-fast freezing methods are presently being explored.

ACKNOWLEDGEMENTS

We are grateful to Drs. R. Fourme and M. Renaud for the use of their cryostat and to Drs. J. Dufourcq, R. Bernon and C. Lusson for providing solutions of cytochrome b_5-lecithin vesicles. This investigation was supported (in part) by a Postdoctoral Fellowship from the National Multiple Sclerosis Society (to M.J.C.), by N.I.H. grant 1 K07 EY 00035-01, and by the Délégation Générale à la Recherche Scientifique et Technique.

REFERENCES

1 Costello, M. J. and Gulik-Krzywicki, T. (1975) Proceedings of the Fifth International Biophysics Congress (Copenhagen)
2 Costello, M. J. and Gulik-Krzywicki, T. (1976) Biophys. J. 16, 103a
3 Singleton, W. S., Gray, M. S., Brown, H. L. and White, J. L. (1965) J. Am. Oil Chem. Soc. 42, 53–56
4 Shechter, E., Letellier, L. and Gulik-Krzywicki, T. (1974) Eur. J. Biochem. 49, 61–76
5 Spatz, L. and Strittmatter, P. (1971) Proc. Natl. Acad. Sci. U.S. 68, 1042–1046
6 Deamer, D. W., Leonard, R., Tardieu, A. and Branton, D. (1970) Biochim. Biophys. Acta 219, 47–60
7 Gulik-Krzywicki, T., Shechter, E., Luzzati, V. and Faure, M. (1969) Nature 223, 1116–1121
8 Dufourcq, J., Bernon, R. and Lussan, C. (1976) Biochim. Biophys. Acta 433, 251–263
9 Renaud, M. and Fourme, R. (1967) Acta Cryst. 22, 695–698
10 Gabriel, A. and Dupont, Y. (1972) Rev. Sci. Instrum. 43, 1600–1602
11 Weast, R. C., ed. (1968) Handbook of Chemistry and Physics, 48th edn., p. F-1, Chemical Rubber Company, Cleveland, Ohio
12 Dowell, L. G., Moline, S. W. and Rinfret, A. P. (1962) Biochim. Biophys. Acta 59, 158–167
13 Kléman, M., Williams, C., Costello, M. J. and Gulik-Krzywicki, T. (1976) Defect Structures in Lyotropic Smectic Phases Revealed by Freeze-Fracture Electron Microscopy, Phil. Mag., in the press

14 Ranck, J. L., Mateu, L., Sadler, D. M., Tardieu, A., Gulik-Krzywicki, T. and Luzzati, V. (1974) J. Mol. Biol. 85, 249–277
15 Gulik-Krzywicki, T. (1975) Biochim. Biophys. Acta 415, 1–28
16 Dupont, Y., Harrison, S. C. and Hasselbach, W. (1973) Nature 244, 555–558
17 Costello, M. J. and Bank, H. (1975) Proceedings of the Twelfth Annual Meeting of the Society of Cryobiology (Washington, D. C.)